Numerical Simulation of Temperature and Stress Fields in the Rock Heating Experiment

Author P. Rálek[1*], M. Hokr[1]
[1]Technical University of Liberec, Liberec, Czech Republic
*Corresponding author: petr.ralek@tul.cz

Abstract: The presented work is motivated by pre-realization phase of rock heating experiment in underground, testing the rock properties for cyclic energy storage. Heating unit, installed in large borehole from end of a tunnel, is fixed to the rock face with the geo-polymer. The rest of the borehole is filled with the isolation material. We used the Heat Transfer Module and the Structural Mechanics Module in COMSOL for modeling of the transient heat conduction with thermo-elasticity in 3D, both with parametrized material properties. The objective of the work was to predict the temperature distribution and induced mechanical stresses in the area close to the heater, in order to set working range of sensors placed in measuring boreholes spread around the main borehole. The largest mechanical loading emerges on heater-geopolymer-rock interfaces, but the general shape of the temperature and stress field outside the borehole is mostly influenced by properties of the rock.

Keywords: heat transfer, thermo-elasticity, rock heating, geothermal, energy storage.

1. Introduction

The presented work is motivated by preparation and calibration of rock heating experiment in underground, for testing the rock properties for geothermal application, particularly cyclic energy storage [1, 2]. The experiment is placed at the Underground Laboratory Josef in Central Bohemia [3] and adapts the concept of former experiments like [4, 5] to local conditions and particular application. The objective of the work was to predict the distribution and range of the temperature (which for simpler geometry was presented in [6]) and newly the induced mechanical stresses in the area close to the heater. The results served for setting the working range of mechanical and temperature sensors, placed in several testing boreholes.

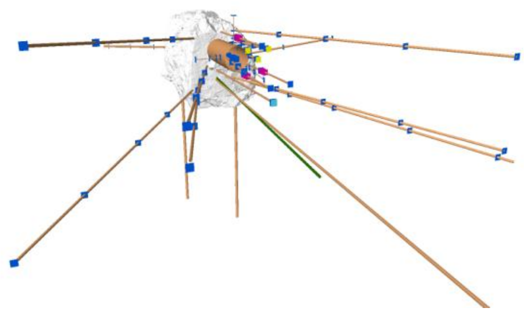

Figure 1. GIS visualization of part of the tunnel with main borehole and sensor boreholes (blue squares show sensors placement).

1.1 Experiment

Large borehole, 0.86m wide and 2.5m long, was drilled in the tunnel heading. Its first part, 2m long, is filled by isolation and, through its central part, the heated water pipe transports the 90°C hot water to the heating unit (Fig. 3). The contact between the heating unit and the rock is made by special thermal-conductive geo-polymer layer.

The neighborhood of the main borehole is covered with the measuring boreholes (from 0.06m to 0.076m wide, with different length and orientation), where the sensors are placed (Fig. 1). The interior of the sensor boreholes is also filled with isolation.

Both processes of heating and cooling (when the heating will be switched off) will be observed.

1.2 Model geometry

In the model, some simplification of the reality was made. We consider, that the tunnel has a strictly symmetrical shape (Fig. 2). The model domain is a cube with 20m long side, without the 10m long part of the tunnel (empty space). The dimensions are considered to exceed the rock volume influenced by the experiment, which was confirmed by the previous simulation results [6].

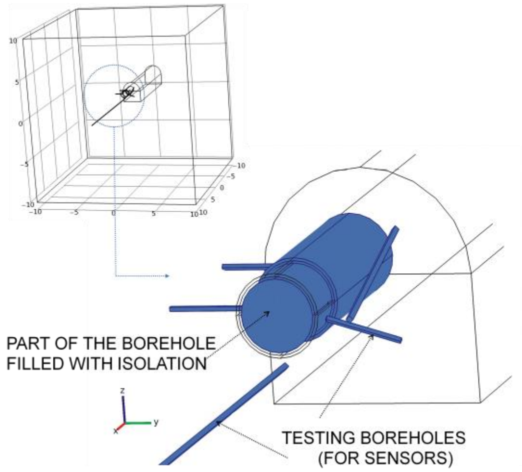

Figure 2. Model geometry (isolation is marked by blue color).

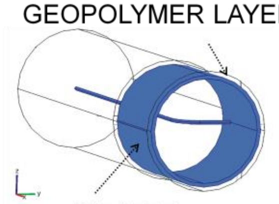

Figure 3. Geometry of the heating unit inside the borehole (marked blue).

The sensor boreholes are positioned and oriented according to the reality.

All geometric properties are used as parameters (to be finally arranged according to the experiment, after finishing of drilling and heater mounting). Material properties of the granite rock and developed geo-polymer are obtained from measurement.

3. Numerical solution

The modeled process is the unsteady heat conduction in solid with thermo-elasticity. At the boundaries of the tunnel, we suppose the convective cooling. At the boundaries of the whole cubic domain, we suppose to be no influence of the heating process (constant rock temperature).

3.1 Governing equation

The unsteady heat conduction with thermo-elasticity is described by the governing equation

$$\varrho C_p \frac{\partial T}{\partial t} + T \frac{\partial}{\partial t} S_{elast} = \nabla \cdot (k \nabla T) + Q_h$$

where T is the temperature, C_P is the heat capacity under the constant pressure, S_{elast} is the deformation tensor, k is the thermal conductivity, ρ is the density, t is the time and Q_h is the heat source. Boundary conditions are

$$T = T_0 \quad on\ \partial\Omega_D$$

where Ω_D is the external boundary of the cubic domain. For the tunnel sides, we prescribe the heat transfer

$$\mathbf{n} \cdot (k \nabla T) = h_x (T_1 - T) \quad on\ \partial\Omega_x$$

where Ω_x is a part of the tunnel boundary and h_x is the corresponding heat transfer coefficient (x = "head" for the tunnel heading, x = "sides" for the bottom and sides of the tunnel), **n** is normal vector of the boundary, T_0 is prescribed temperature of the granite massif, T_1 is prescribed air temperature inside the tunnel. We distinguish the heat transfer at the tunnel heading (where an isolation layer can be used) and at the remaining sides of the tunnel (where the heat transfer is influenced only by ventilation).

3.2 COMSOL solution

In the COMSOL Multiphysics, we created a study with two steps. Step 1 used the Heat Transfer module (particularly, heat transfer in solids with convective cooling inside the tunnel). Step 2 used Solid mechanics module (particularly thermal expansion and linear elasticity).

We present the stationary studies to observe the steady state of the heating process, when the greatest stress response of the rock to the heating is assumed.

4. Results

4.1 Visualization

In the post-processing stage, line profiles (Fig. 4) are presented to analyze the rate of temperature and pressure drop in directions along various measuring boreholes. Colors of the lines on Fig. 4 correspond to the colors used in the graphs in the Appendix. We chose to display

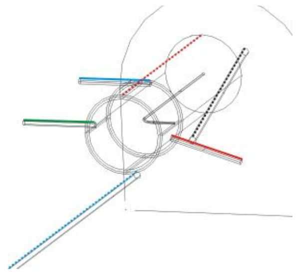

Figure 4. Lines selected for the line graphs.

the pressure instead of stress field due to its simplicity (scalar values instead of components of vector field). Beside the lines graphs, we present 2D slices.

4.2 Temperature distribution

The temperature range in 1m surroundings of the main borehole is from 80°C to 27°C (Fig. 7, 10). Along transversal sensor bore holes (each 80cm long), drops the temperature roughly exponentially from 80°C to 31°C (Fig. 5). For preserving the similar temperature change between two sensors in the borehole, each sensor should have double distance from the main borehole than the preceding one.

Along longitudinal boreholes, the temperature decreases in both directions from maximal values near the heating unit (different for each borehole) to common minimum 10°C (Fig. 6). The drop is much faster in direction to the tunnel heading (where we assume convective cooling), therefore the sensors should be distributed densely in this part of bore holes.

4.3 Stress distribution

Stress field in transversal cross-section has similar shape to the temperature (Fig. 8, 12). From maximal values about $5x10^7$ $N.m^{-2}$ (attained in *z* direction) drops the stress exponentially to about $5x10^6$ $N.m^{-2}$ in 1m surroundings.

In longitudinal directions, the drop is also faster in direction to the tunnel heading (Fig. 9). Biggest stress leaps occur at the heater-geopolymer-rock interfaces. Outside the main borehole, the stress field dependes on the properties of the rock.

5. Conclusions

The results describe well the range of temperature and pressure in the area close to the borehole, where the sensors will be installed (Fig. 6-7). Temperature, in 1m surroundings, decreases from 90°C to about 30°C. The thermal-induced stress has complicated distribution very near the heater body and testing boreholes. Pressure, in 1m surroundings, decreases from 50 MPa to about 5MPa.

The general shape of the temperature and stress field outside the borehole is influenced primarily by properties of the rock.

6. References

1. H. Hokmark, B. Falth, Thermal dimensioning of the deep repository. Influence of canister spacing, canister power, rock thermal properties and near field design on the maximum canister surface temperature, *SKB report*, **TR-03-09** (2003)
2. H.F Zhang, X.S. Ge, H. Ye, Modeling of a space heating and cooling system with seasonal energy storage, *Energy*, **32**, p. 51–58 (2007)
3. The JOSEF Underground Laboratory, Czech Technical University, http://www.uef-josef.eu/ (2011)
4. E. Detournay, T. Senjuntichai, I. Berchenko, An in situ thermo–hydraulic experiment in a saturated granite II: analysis and parameter estimation, *Int. J. Rock Mech. Min. Sci.*, **41**, p. 1395–1411 (2004)
5. I. Javandel, P.A. Witherspoon, *Thermal Analysis of the Strip Heater Test Data From the Full Scale Drift*, 124 pp., Lawrence Berkeley National Laboratory, LBNL-13217, (1981)
6. M. Hokr, P. Rálek, Numerical Simulation for Dimensioning a Rock Heating Experiment, 7 pp., *COMSOL Conference Stuttgart 2011 Proceedings CD* (2011)

7. Acknowledgement

This work was realized under the state subsidy of the Czech Republic within the research project FR-TI3/325 supported by Ministry of Industry and Trade.

8. Appendix – results

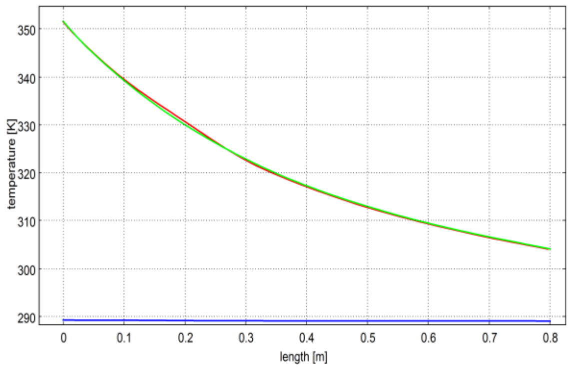

Figure 5. Temperature drop along transverse measuring boreholes.

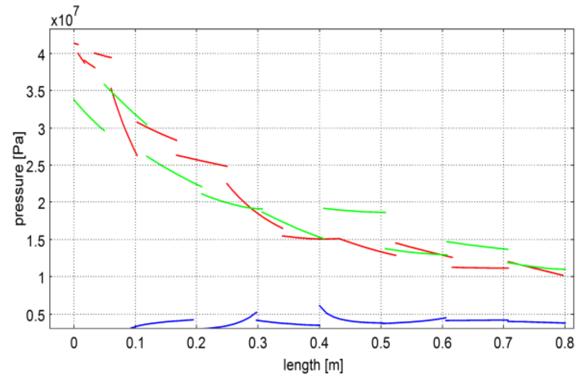

Figure 8. Pressure drop along transverse measuring boreholes.

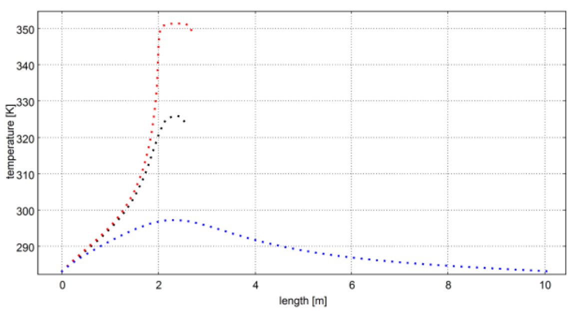

Figure 6. Temperature drop along longitudinal measuring boreholes.

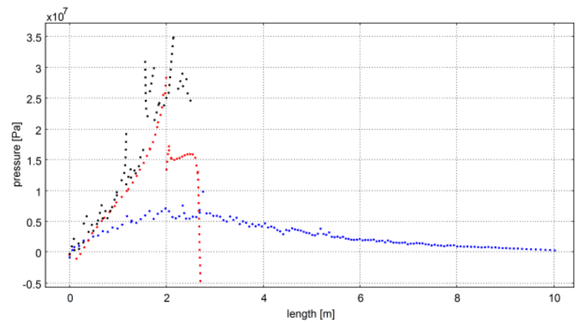

Figure 9. Pressure drop along longitudinal measuring boreholes.

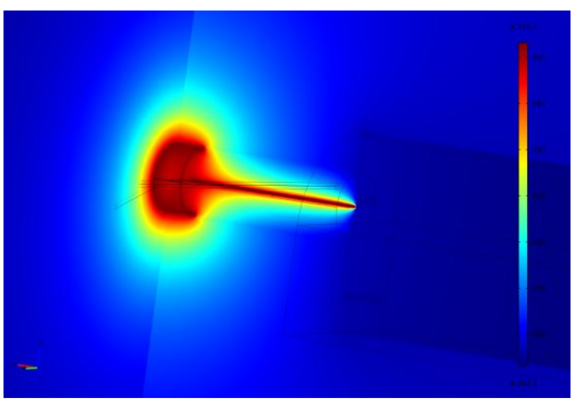

Figure 7. Combined slices of temperature field [K].

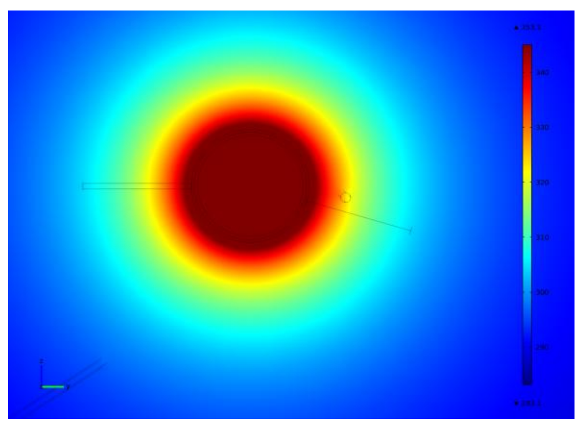

Figure 10. Frontal slice of temperature field [K].

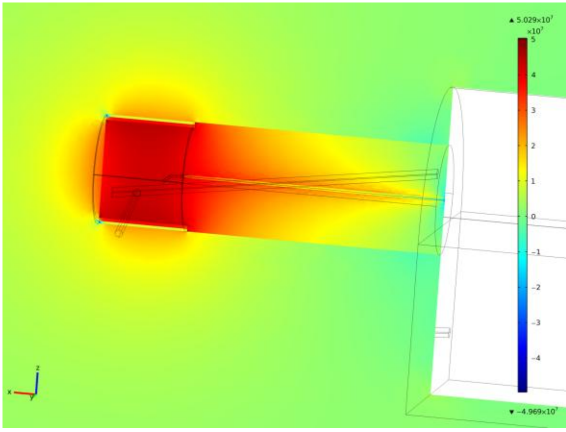

Figure 11. Lateral slice of pressure field [Pa].

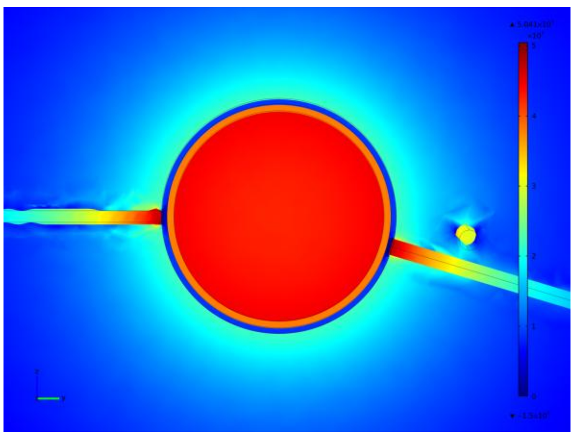

Figure 12. Frontal slice of pressure field [Pa].

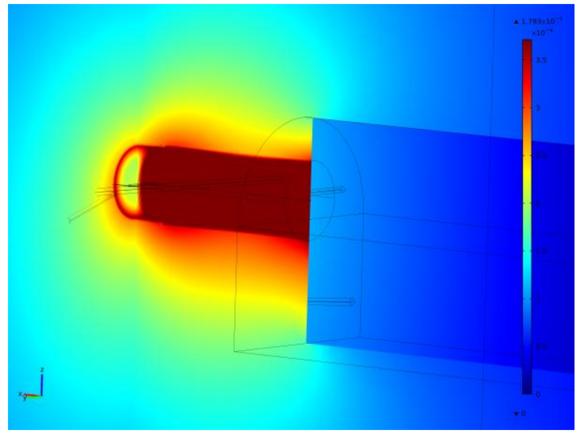

Figure 13. Lateral slice of displacement field [m].

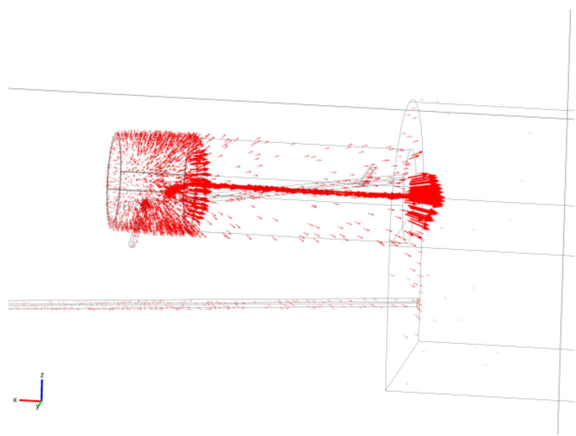

Figure 14. Arrow surface of displacement field [m].